The Active State of Supported Ruthenium Oxide Nanoparticles during Carbon Dioxide Methanation

Sophie Carenco,[1,2,] Capucine Sassoye,[1] Marco Faustini,[1] Pierre Eloy,[3] Damien P. Debecker,[3] Hendrik Bluhm,[2] Miquel Salmeron[4]*

[1] Sorbonne Universités, UPMC Univ Paris 06, CNRS, Collège de France, Laboratoire de Chimie de la Matière Condensée de Paris, 11 place Marcelin Berthelot, 75005 Paris, France

[2] Chemical Sciences Division, Lawrence Berkeley National Lab, Berkeley, California, United States.

[3] Institute of Condensed Matter and Nanoscience – MOlecules, Solids and reactiviTy (IMCN / MOST). Université catholique de Louvain. Croix du Sud 2 box L7.05.17, 1348 Louvain-La-Neuve, Belgium.

[4] Material Sciences Division, Lawrence Berkeley National Lab, Berkeley, California, United States.

E-mail: sophie.carenco@upmc.fr

Abstract:

Ruthenium catalysts supported on TiO_2 are shown to have interesting activity and selectivity for the methanation of CO_2. In particular, a catalyst using pre-formed RuO_2 nanoparticles deposited on the TiO_2 support, showed competitive performances in a previous study. Here, near-ambient-pressure X-ray photoelectron spectroscopy was employed to provide a description of this catalyst under reaction conditions. The active state of ruthenium was shown to be the metallic one. Surface reaction intermediates were monitored at the steady state, and CH_x species were found to be favored over adsorbed carbon monoxide upon temperature increase.

Key-words: ruthenium nanoparticles, ambient-pressure XPS, carbon dioxide, CO_2 hydrogenation, active state.

1. Introduction

Ruthenium-based nanoparticles are highly efficient catalysts for a range of reactions: ammonia synthesis,[1,2] oxidation of volatile organic compounds,[3],[4] methane dry reforming,[5] carbon monoxide oxidation,[6] HCl oxidation.[7,8],[9,10] Amongst them, the methanation of carbon dioxide, also known as the Sabatier reaction, is currently attracting attention because of its relevance to the field of chemical energy storage.[11] The support of the nanoparticles catalysts was shown to have performance by affecting its dispersion and also its robustness towards coking.[12] TiO_2 supports have emerged as promising ones to enhance the stability of Ru-based methanation catalysts.

Despites its economic importance, the Sabatier reaction still lacks a full description in terms of surface state of the catalyst exposed to the reactive gases. For supported ruthenium catalysts, previous mechanistic studies were conducted using temperature-programmed adsorption and reaction,[13] Fourier-transformed infra-red (FTIR) spectroscopy,[14],[15] as well as transient mass-spectrometry.[16] These studies were conducted on catalysts prepared by wet impregnation of a Ru salt (generally $RuCl_3$), on TiO_2 or other supports.[5],[17] It is believed that CO_2 adsorption is thermally activated and results in formates and CO species.[16] CO further reacts with surface hydrogen to yield CH_x and eventually methane. Besides, it was shown by Panagiotopoulou et al. that under methanation conditions, CO_2 does not dissociate all the way to adsorbed carbon and oxygen on Ru/TiO_2.[15]

In a previous work, we developed a green route to small RuO_2 nanoparticles of 2 nm diameter.[18] The nanoparticles were impregnated on TiO_2-P25 support, annealed, reduced and tested for the methanation of CO_2 at 200 °C. They were found to be more active than a reference Ru/TiO_2 catalyst prepared by wet impregnation of the support with $RuCl_3$.

The active state of the surface, when exposed to the reactive gas mixture, has not yet been determined on this new catalyst. While traditional X-ray photoelectron spectroscopy (XPS) can only be conducted

under ultra-high vacuum (UHV), so-called ambient-pressure XPS (APXPS), developed in the last decade, allows analyzing a surface exposed to a few mbar of gas. While this pressure is still below the typical operating pressure for the Sabatier reaction (1 bar), it is high enough to ensure the saturation of surface sites with adsorbates, thus making the measurement representative of the surface steady state in the catalytic reactor. This was demonstrated on a number of metal and metal oxide catalysts in the past ten years and by several groups,[19–28] and in particular for the reaction of catalytic CO oxidation on bulk ruthenium oxide.[29]

In this paper, we monitored the surface state of a RuO_2/TiO_2 catalyst whose excellent activity and selectivity in CO_2 methanation was demonstrated in prior works. Two types of catalysts were studied: (i) a model surface of TiO_2 onto which the RuO_2 nanoparticles were deposited, and (ii) the actual catalyst powder (RuO_2 nanoparticles impregnated on TiO_2-P25). We followed the reduction process leading to active metallic ruthenium nanoparticles and we further characterized the state of the surface exposed to CO_2/H_2 gas mixtures (1:4 ratio and total pressure of 0.33 mbar). Our main findings are that, under model reaction conditions, (i) the ruthenium stays metallic, and (ii) upon temperature increase the surface is depleted of carbon-oxygen species in favor of C-(C,H) species. These results were validated both on the model surface and on the real catalyst.

2. Results

2.1 Study of the Model Surface

Design of a thin film supported model sample:

Because TiO_2 powder is a non-conductive substrate, preliminary studies of RuO_2 on TiO_2-P25 showed inhomogeneous charging effect of the surface that hampered the collection of exploitable data. A model surface was designed to circumvent this problem (Scheme 1). A thin layer of TiO_2 perforated with regularly spaced holes was deposited on a gold surface, following a sol-gel route developed in our group.[30] The holes were disposed in a 2D pseudo-hexagonal arrangement with an average hole diameter of 17 nm and an average center-to-center distance of 25 nm. The thickness of the TiO_2 film

was 7 nm,[31] which is larger than electron mean free path of XPS (< 2 nm). The gold under-layer provided electronic conductivity to the sample as well as an XPS reference using the Au 4f doublet at 84 eV that could be measured on the exposed gold (in the holes). The TiO_2 perforated layer contains both anatase and more amorphous phases, according to previous studies. RuO_2 nanoparticles of 2 nm diameter were prepared following a colloidal aqueous route described in a previous work.[18] They were deposited on this model surface by dip-coating from a colloidal solution in water/ethanol. In this geometry, the nanoparticles of RuO_2 are sitting on the TiO_2 layer and the gold surface. The thin film was calcined at the temperature used for the real catalyst: 450 °C.

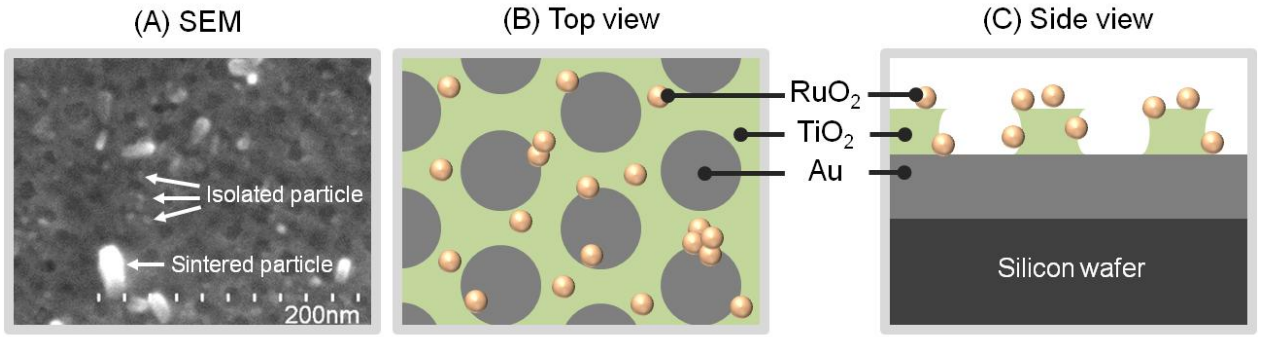

Scheme 1: (A) Scanning Electron Microscopy of the thin film surface (Top view). Top view (B) and side view (C) of the model catalyst surface.

Geometrical factors alone do not ensure that all RuO_2 nanoparticles are in contact with the TiO_2 layer. After evaporation of the ethanol, the remaining water-rich solution preferentially wets TiO_2 and, as a result, RuO_2 nanoparticles are concentrated on TiO_2. Selective deposition on similar chemical heterogeneous supports was previously observed for FePt particles.[32] The thin film was optically flat, indicating a surface roughness lower than 50 nm. Top-view provided by field-emission scanning electron microscopy (FEG-SEM) showed good homogeneity at a 100 nm scale (Scheme 1A), which is far below the X-Ray beam size of XPS (ca 100 µm). Although some sintered RuO_2 nanoparticles can be observed (see also Figure S1A), most of the surface is covered with RuO_2 nanoparticles of small diameter (2-5 nm) that are observed by SEM as small bright dots at the limits of the apparatus resolution. The sintered particles were due to the calcination of the thin film (see Figure S1A). Due to

their limited number and surface coverage, their contribution to the XP spectra was considered to be negligible (see the discussion section).

Overall, this sample geometry provided the adequate intimate contact between RuO_2 and TiO_2 while avoiding charging effects, thanks to the gold under-layer that is conductive and chemically inert.

Initial state of the RuO_2 nanoparticles on the model surface

The model surface with RuO_2 nanoparticles was introduced in the APXPS chamber at BL11.0.2 of the *Advanced Light Source*, Berkeley.[33]

As expected from the design of the model surface, no significant charging effect was observed on any point of the sample. Data could be collected with the expected resolution of ca 0.1 eV typical of the beamline, and no beam damage effect was observed.

XPS measured with photon energy of 700 eV showed a complex signal in the region of interest (276-294 eV). The initial state of the surface was assessed under UHV (Figure 1a). In particular, the contribution of a wide Ti_{LMV} Auger peak (in black on Figure 1a) has to be subtracted for the proper decomposition of the C1s and Ru3d core level spectrum. It was modeled with CasaXPS software package[35] using two components of apparent binding energies 281.5 and 286.6 eV whose shapes are a product of Gaussian and Lorenzian functions (see Supplementary information).[34]

Metallic Ru was fitted using a Gaussian-Lorenzian product formula modified by an exponential blend. This shape was chosen over a Doniach-Sunjic profile because if fitted extremely well the fully reduced spectra, at all photon energies. Metallic Ru is represented with an asymmetric line shape doublet at 280.0 eV while the oxidized Ru species are described with the combination of a main doublet (~280.8 eV) accompanied by a satellite doublet (282.4 eV). Each of them was simulated with two symmetric Gaussian-Lorenzian functions separated of 4.17 eV and with the expected area ratio of 3:2. About 1.6 eV separated the satellite and the main doublet. Their ratio was close to 50%, in agreement with recent work of D.J. Morgan.[36] C1s components, which overlap with $Ru3d_{3/2}$ components, were fitted

with Gaussian-Lorenzian functions with FWHM and binding energy parameters consistent through all the spectra (see Supplementary Information).

After introduction of the thin film in the UHV chamber, ruthenium was found to be essentially oxidized, as expected (blue components at 280.8 eV for $Ru3d_{5/2}$ and 285.0 eV for $Ru3d_{3/2}$). Only 11% of the Ru was in a reduced form (red components at 280.0 eV for $Ru3d_{5/2}$ and 284.2 eV for $Ru3d_{3/2}$).

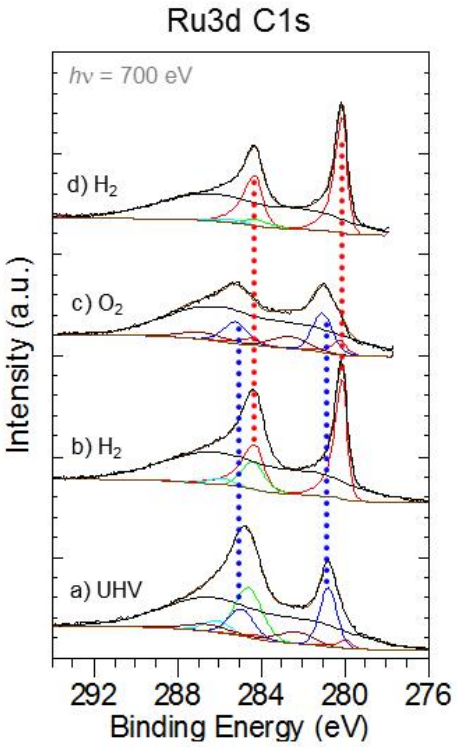

Species		B.E. (eV)	FWHM (eV)	Color
Ru(0)	$Ru3d_{5/2}$	280.0	0.6	Red
	$Ru3d_{3/2}$	284.2	0.9	Red
RuO_x	$Ru3d_{5/2}$	280.8	0.9	Blue
	$Ru3d_{5/2}$ sat.	282.4	2.0	Brown
	$Ru3d_{3/2}$	285.0	1.4	Blue
	$Ru3d_{3/2}$ sat.	286.6	2.5	Brown
C1s	C-(C,H)	284.6	1.5	Green
	C-O	286.2	1.5	Light blue
Ti LMV	$L_3(Ti)M_{23}$ (Ti)V(Ti)	(281.5)*	5.5	Black
	$L_3(Ti)M_{23}$ (Ti)V(O)	(286.6)*	5.5	

* Apparent binding energy

Figure 1: (Left) XPS under UHV of RuO_2 nanoparticles on model surface: (a) Thin film after introduction in the UHV chamber, (b) after first treatment under H_2 (250 °C), (c) after treatment under O_2 (200 °C), (d) after second treatment under H_2 (200 °C). Red dotted lines indicate Ru(0) species while blue dotted ones indicate oxidized Ru. Spectra were collected with a photon energy of 700 eV. (Right) Decomposition parameters.

These observations were repeated using other photon energies of 620, 700, 875 and 1115 eV (Figure 2A), representing mean free path of respectively 0.57, 0.63, 0.81 and 1.0 nm, according to Cumpson and Seah,[37] and assuming that electrons are ejected from metallic ruthenium. Although accurate models for evaluating mean free paths are still the object of active research,[38,39] the trend is significant, as a lower photon energy ejects photo-electron with lower kinetic energy. Thus, spectrum (a) on Figure 2

corresponds to near surface composition, while spectra (b), (c) and (d) represent deeper layers. All spectra of the initial state of the film, after its introduction in the UHV chamber (A), are similar, indicating that the structure of the RuO_2 nanoparticles is homogeneous from core to shell.

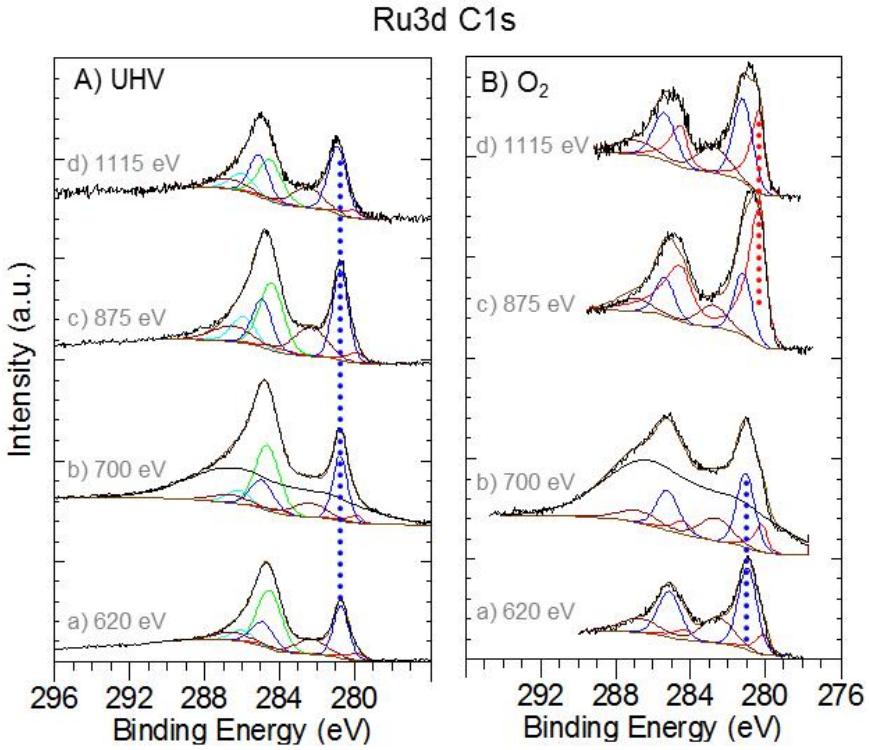

Figure 2: XPS of RuO_2 nanoparticles on model surface using several photon energies: (A) initial state of the film and (B) after the sequence of reduction and oxidation. Dotted lines are a guide to the eye: red ones indicate Ru(0) species while blue ones indicate oxidized Ru.

Reduction of the RuO_2 nanoparticles on the model surface

In order to simulate the treatments conducted in a real catalytic reactor, the RuO_2 nanoparticles on the model TiO_2 surface was exposed to H_2 (6 mbar) and heated to 250 °C. Within minutes, complete reduction of Ru to Ru(0) was observed, as shown by the disappearance of the doublet at 280.8 eV on spectrum (b) of Figure 1. This demonstrates that the nanoparticle surface is clean and confirms the reducible nature of RuO_2 on TiO_2, which are then used for subsequent reactions with gases.

As a further proof, an additional cycle of oxidation under O_2 (0.7 mbar) at 200 °C, followed by a reduction under H_2 (0.7 mbar) at 200 °C, was performed. After the oxidation, 23 % of Ru remained in a

reduced state as measured from the spectrum collected with a photon energy of 700 eV (Figure 1c and Figure 2B-b). Interestingly, the spectrum most sensitive to the surface (E_{photon} = 620 eV, Figure 2B-a) showed a percentage of about 17% of Ru(0) species, while spectra more sensitive to the bulk showed 71 % (Figure 2B-c) and 44 % (Figure 2B-d) of Ru(0) species.

The higher proportion of surface oxide a lower photon energy indicates that the oxidation of Ru(0) nanoparticles is confined mostly to the surface in these conditions. After subsequent reduction under H_2, all Ru species returned to the metallic state, as can be seen on Figure 1d. On this spectrum, the remaining of few carbon-containing species (both C-(C,H) and C-O) was still observed, and could be adsorbed on Ru, on TiO_2 and/or on the exposed gold surface.

Chemical state under exposure to reactive gas mixtures

Following the reduction step, the sample was exposed to a flow of CO_2 (0.066 mbar) and H_2 (0.264 mbar) in the same 1:4 ratio as in the catalytic reactor.[18] The state of the surface was monitored while increasing the temperature from r.t. to reaction temperature of 200 °C. Spectra are presented on Figure 3A. The high binding-energy peak at 293.1 eV is due to gas-phase CO_2. Ruthenium species stayed in a purely metallic form through the whole process, as attested by the absence of the 280.8 eV peak. Two carbonated species are observed: C-O species at 286.2 eV (light blue on Figure 3) and C-(C,H) species at 284.6 eV (green). Their intensities are higher than those observed on Figure 1, indicating that they result from dosing CO_2 and H_2 in the UHV chamber.

The first one is due to the molecular and/or dissociative adsorption of CO_2, as discussed further below. The second carbonated species, at 284.6 eV, is attributed to CH_x intermediates that form in the way to CH_4 as well as on competitive pathways forming C-C bonds that also occur on a ruthenium catalyst.[40],[41]

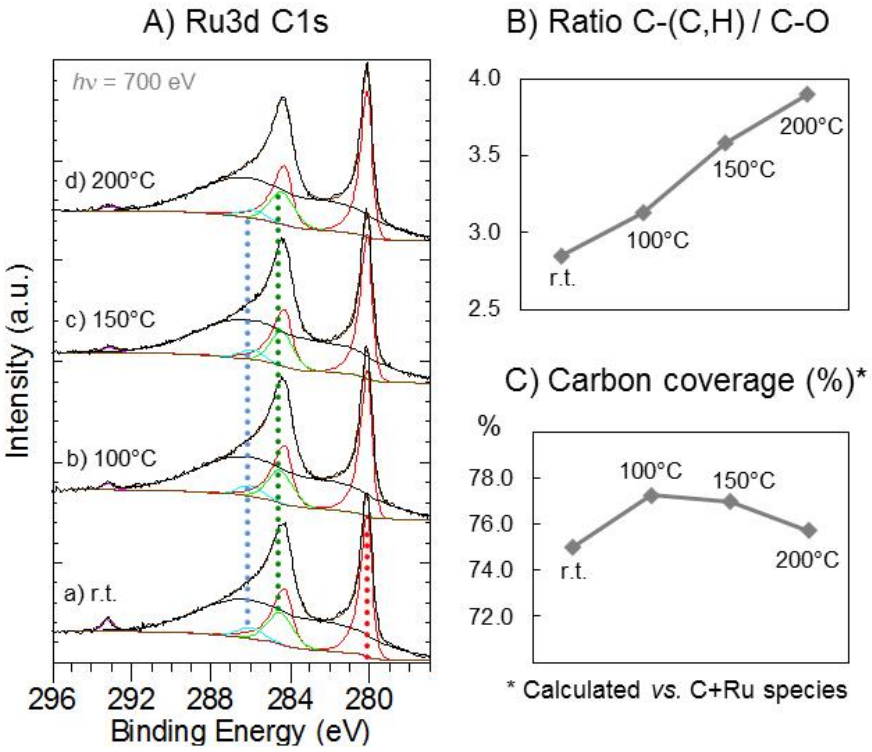

Figure 3: (A) XPS of reduced surface under model catalytic conditions, from r.t. (a) to 200 °C (d). Dotted lines are a guide to the eye: red for Ru(0), light blue for C-O species, green for C-(C,H) species. (B) Ratio of C-(C,H) to C-O species. (C) Carbon (sum of C-O and C-(C,H) species) coverage in %.

The ratio of Ru species to the overall carbon species only slightly evolves from 0.21 to 0.26 through the experiment (not shown). However, upon heating from room temperature to 200 °C, the ratio of C-(C,H) species to C-O species increased by 137 %, from 2.8 to 3.9 (Figure 3B). Two interpretations can be proposed: (i) upon temperature increase, the equilibrium of adsorption-desorption of CO_2 from the gas phase is shifted toward desorption; (ii) upon temperature increase, more C-H and C-C bonds forms at the surface, providing intermediates for CH_4 generation. It is likely that both phenomena contribute to the overall ratio evolution because (i) the first one is well-established in general on any surface, and (ii) in the catalytic reactor, increasing the reaction temperature does increase the rate of methane formation.

Lastly, the carbon surface coverage (calculated vs. the sum of carbon and ruthenium species) remains stable, in the range of 75-78 % (Figure 3C). This indicates that there is no carbon built-up during the reaction at 200 °C, although a small increase in carbon content is observed at lower temperature of 100 and 150 °C. This indicates that formation of C-C chains is disfavored over CH_4 formation when

increasing the temperature, because the first would stay longer on the surface while the latter is desorbed to the gas phase.

Altogether, this experiment demonstrated that, on this TiO_2 support, (i) the ruthenium stays metallic in the reaction conditions used here, and (ii) full hydrogenation to methane is favored.

Interaction of CO_2 with the surface

Complementary experiments were conducted, in order to gain information on the adsorption of CO_2 on the nanoparticles. On the reduced surface, CO_2 was introduced in the chamber, without hydrogen gas. The surface was either kept at r.t. under 0.66 mbar (Figure 4A) or heated to 250 °C under 4.0 mbar (Figure 4B). After cooling the sample and pumping the gas, spectra were collected in UHV. It was found that ruthenium remained reduced and in similar relative amount in both experiments. The carbon content was slightly decreased, by 6 % at r.t. and by 8 % at 250 °C. However, a three-fold increase of the ratio C-O/C-(C,H) was observed for the reaction at r.t (Figure 4C). At 250 °C, the increase was even more pronounced (Figure 4D).

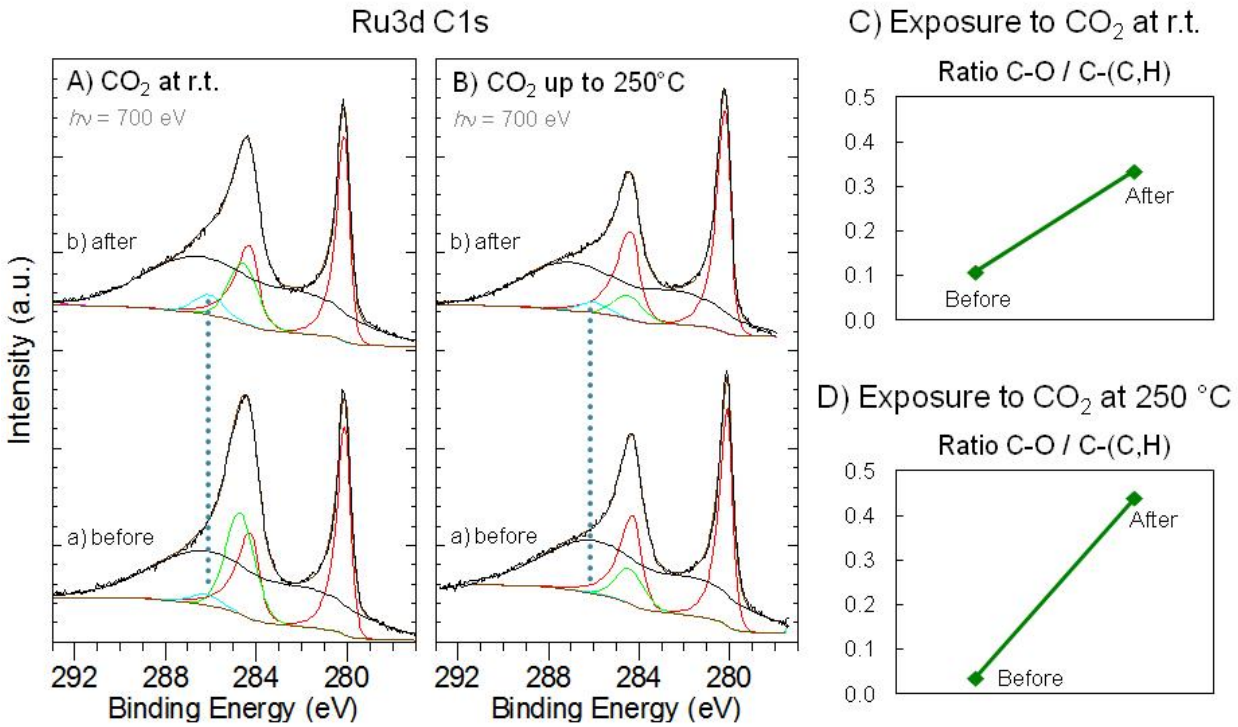

Figure 4: (Left) XPS in UHV at r.t. (A) and at 250 °C (B), before (a) and after (b) exposing the surface to CO_2 gas. Dotted lines are a guide to the eye, indicating the B.E. of C-O species. (Right) Ratio of C-O species to C-(C,H) species at r.t. (C) and at 250 °C (D).

2.2 Comparison with the real catalyst powder (RuO_2 on TiO_2-P25)

In order to validate our study on the model surface, we attempted a comparison with the actual powder used as the catalyst of CO_2 methanation. This powder is prepared by impregnation of the same RuO_2 nanoparticles, on TiO_2-P25 from Degussa.[18] Two features make this catalyst difficult to analyze by XPS. TiO_2 powder became electrically charged upon exposure to X-Ray: to remediate this, we choose gold as a substrate for depositing a thin layer of the RuO_2/TiO_2-P25 powder (Figure 5A). There are still charging effects on some parts of the surface but others show no charging, allowing to collect data. The second difficulty is the lower loading of Ru on this sample: ca 2%. This required longer counting times (~50 times more), to detect the ruthenium.

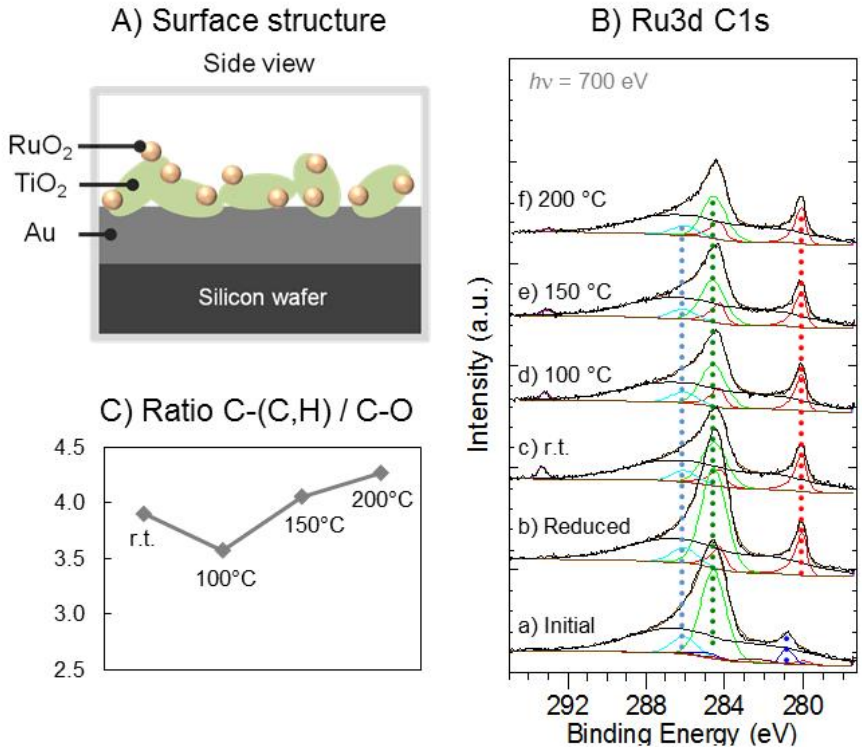

Figure 5: (A) Side view of the real catalyst powder deposited on Au surface. (B) XPS of the catalyst powder deposited on gold: (a) under UHV, initial state, (b) under UHV, after reduction by H_2 at 250 °C, (c)-(f) under model catalytic conditions (CO_2:H_2 in 1:4 ratio), from r.t. to 200 °C. Dotted lines are a guide to the eye: red for Ru(0), dark blue for oxidized Ru, green for C-(C,H) species and light blue for C-O species. (C) Ratio of C-(C,H) to C-O species during the reaction.

The catalyst was reduced under H_2 (6 mbar) at 250 °C, then exposed to the reactive gas mixture (CO_2 and H_2 in a 1:4 volumetric ratio, 0.33 mbar total pressure). The temperature was increased from r.t. to 200 °C. XPS is presented on Figure 5B. Although Ru is more difficult to detect than on the model surface, these data confirmed the observations made previously. Figure 5B-b showed that ruthenium was fully reduced upon H_2 treatment. Figure 5B-(c-f) showed that ruthenium stays metallic under reaction conditions, and that there is no built-up of carbonated species on the surface. As observed for the model surface, under reaction conditions the C-O species are disfavored over C-H and C-C species (Figure 5C), although this is less significant here. Overall, observations on the real catalyst powder confirmed the trends discussed in detail on the model surface.

3. Discussion

3.1 Design of the model surface

The first part of this study presented data obtained with RuO_2 nanoparticles deposited on a perforated thin film of TiO_2, which was itself supported on a conducting and chemically inert gold layer. This geometry proved efficient to collect good quality XPS without encountering spectroscopic limitations such as charging of the surface. Calibration on Au4f rather than on adventitious carbon was important because of the overlap of Ru3d and C1s regions.

The TiO_2 of this layer is composed of anatase as well as amorphous TiO_2. The support used in the catalytic reaction, TiO_2-P25, is also mostly made of anatase (ca 78 %) and amorphous TiO_2 (ca 8 %) but it contains rutile (ca 14%).[42] It was recently uncovered that rutile, better than anatase, prevents the aggregation of RuO_2 nanoparticles during calcination in air.[12] Although the thin film was calcined only for five minutes, the presence of a few sintered RuO_2 particles on our thin film (Scheme 1 and Figure S1A) was expected. However, we found this not to be an issue here because: (i) the total surface covered by these particles being of a few %, their contribution to the XP spectrum is not significant, and (ii) the sintering did not progress during the catalysis step (Figure S1B).

The use of the model surface was also supported by the fact that the two main observations of this study were consistent with those on the real catalyst: ruthenium is metallic at 200 °C under CO_2 and H_2, and the C-(C,H) species are favored over the C-O species.

Use of this perforated film allowed collecting high-quality data in a limited time, thanks to the absence of any charging effect and of the fairly high loading of ruthenium (ca 0.2 monolayer) allowed by this sample geometry. It allowed for an in-depth analysis of the surface composition, including depth profiling. This strategy of perforated thin film[30,43] could be applied to other nanoparticles that are supported on metal oxides (eg. ZrO_2, Al_2O_3, mixed oxides) in a catalytic reactor.

3.2 Oxidation state of ruthenium

The oxidation state of ruthenium was analyzed at each stage, both on the model surface and on the

real catalyst powder. XPS at Ru 3d level allows resolving the oxidation states of Ru.[44] As expected, Ru was found to be oxidized on the calcined sample (Figure 1a, Figure 5B-a) but easily reduced under H_2 at 250 °C to a fully metallic state (Figure 1b, Figure 5B-b). Contrarily to other preparation routes,[45] RuO_2 preformed nanoparticles on TiO_2 were fully reduced under H_2 and no oxidized ruthenium sites was observed at the interface with the oxide, as shown by the fully reduced state observed on Figure 1d.

In the XPS chamber, the nanoparticles were exposed to a mixture of CO_2 and H_2 (ratio 1:4), while spectra were collected. Upon increase of temperature from r.t. to 200 °C, Ru stayed reduced both on the model surface (Figure 3A) and on the catalyst powder (Figure 5B-c-f). This confirmed that the active species is the metallic one, as generally postulated in CO_2 methanation studies,[17] and consistently with observation made in CO methanation reaction.[15] In other studies, on a catalyst prepared by wet impregnation of $RuCl_3$, some $Ru^{(+3)}$-CO were suggested by diffuse-reflectance infrared Fourier transform spectroscopy (DRIFTS), and the occurrence of RuO_x islands was hypothesized at 110 °C.[14] None of these species could be identified in our study, either because they existed at levels below the detection limit of XPS (ca 1%) or because they were simply absent at our reaction temperature of 200 °C.

The metallic state of Ru relates to the reductive conditions used in the methanation reaction, while in more oxidative processes of CO oxidation[6],[46] and methane partial oxidation,[47] oxidized ruthenium were identified as the active species.

3.3 Nature and evolution of surface adsorbates

Previous DRIFTS studies allowed the detection of several carbonated surface species, on the surface of Ru/TiO_2 catalysts at the steady state, including CO, formate, and carbonate. It has been proposed that CO adsorbs on Ru sites while the other species are mostly located on the TiO_2 support.[14,15] Adsorbed CO is expected to have C peak with B.E. of ca 286 eV[48] and formate and carbonate at ca 288-289 eV. On both the model surface and the catalyst powder, our spectra show the presence of CO species fitted by a component at 286.2 eV (Figure 3A, Figure 5B), corresponding to adsorbed carbon monoxide. No

significant amount of formate and carbonate was detected, at the photon energies used (620, 700, 875 or 1115 eV), but the presence of a few percent of a monolayer cannot be excluded on our spectra because their contribution would be strongly overlapping with tail of the asymmetric shape of the $Ru3d_{3/2}$ component, which hinders the analysis.

Besides, no molecularly adsorbed CO_2 was expected, based on DRIFTS measurements reported in other works,[15] and none was detected by XPS in this study. These results indicate that adsorption of CO_2 is an activated process,[13] leading to dissociation into carbon monoxide and oxygen.[14] In order to verify this, the reduced surface was exposed to CO_2 alone (0.66 mbar) either at r.t. or at 250 °C (Figure 4). In both cases an increase in the contribution of surface carbon monoxide was observed, indicating that the adsorption of CO_2 lead to partial dissociation into CO and adsorbed oxygen. The phenomenon was more pronounced at 250 °C, consistently with an activated process.

Under CO_2 and H_2 mixtures, the total carbon content on the surface did not change significantly (Figure 3C). However, upon heating, an increase of the C-(C,H)/C-O ratio was observed both on the model surface (Figure 3B) and on the real catalyst (Figure 5C). C-(C,H) species represent the direct hydrogenation products of CO, i.e. reaction intermediates in the reaction to form of CH_4. Our observation shows that these species are favored over carbon monoxide on the surface when the temperature increases, consistent with the higher rates of methane production. Lastly, no formation of carbon species in the region 282-284 eV was observed on this surface, which is consistent with the previously observed absence of coking at 200 °C on this catalyst.[18]

4. Conclusion

In this work, the active state of RuO_2/TiO_2 catalyst prepared from pre-formed RuO_2 nanoparticles was investigated. Using APXPS, we found that: (i) the ruthenium is metallic at the steady state under CO_2-H_2 mixtures in the temperature range r.t. - 200 °C, (ii) with increasing temperature, less carbon monoxide is observed on the surface compared with CH_x products.

5. Experimental section

(i) The NPs were prepared according to a previously described aqueous route reported previously.[18]

(ii) *TiO_2 thin film preparation*. The nano-perforated TiO_2 layer was obtained from fresh solutions composed of $TiCl_4$:PB-PEO:H_2O:EtOH in the following respective molar proportions : 1:0.002:42:160. Solution A was prepared by mixing the PB-b-PEO (polybutadiene-b-polyethyleneoxide, MWPB=5500g mol^{-1}, MWPEO=5000 g mol^{-1}, P3017-BdEO, Polymersource) in the water and in ¾ of the amount of ethanol. Solution A was aged at 70°C for 2 hours until the complete dissolution of the PB-b-PEO and then cooled down at room temperature. Solution B, containing $TiCl_4$ and the remaining ethanol, was added to the cooled solution A before being stirred at room temperature for 30 minutes. The films were deposited onto the gold layer by dip-coating using a withdrawal speed of 5 $mm.s^{-1}$ and at a temperature of 40°C, and low relative humidity. The as-formed bi-layer system was then heated at 450°C for 5 minutes to ensure crystallization of the TiO_2 top layer.

(iii) *Deposition of RuO_2 nanoparticles on TiO_2 thin films*. The ruthenia aqueous suspension was mixed with an equal volume of absolute ethanol leading to a stable suspension of ruthenia nanoparticles ([Ru]=0.004M). Ruthenia nanoparticles were deposited onto the TiO_2 perforated thin film by dip-coating using a withdrawal speed of 5 $mm.s^{-1}$ at a temperature of 80°C in a dry atmosphere. The as-formed layer was then heated at 450°C for 30 seconds to ensure crystallization RuO_2, following a previously described procedure.[49]

(iv) *Deposition of a thin film of the RuO_2/TiO_2-P25 catalyst powder*. TiO_2 P25 was added to the ruthenia aqueous suspension at room temperature. After evaporation of the water at 50°C under vacuum, the dry powder was heated in air at 150°C for 5 hours leading to a Ru supported catalyst at 2%w on TiO_2. 0.1g of the catalyst powder was added to absolute ethanol (10 mL). After ultrasonification of the suspension, a catalyst thin film was deposited on a gold substrate by dip-coating using a withdrawal speed of 3.3 $mm.s^{-1}$ at room temperature in a dry atmosphere. The as-formed layer was then heated at 450°C for 30 seconds to ensure crystallization RuO_2.

(v) Chemical state of the surface of the nanoparticles was analyzed *in situ* by ambient-pressure x-ray photoelectron spectroscopy (APXPS), which allows exposure of the nanoparticles to gas up to a few Torr. The experiments were conducted at beamline 11.0.2 of the Advanced Light Source in Berkeley, California. Au4f and Au4d peaks were used to calibrate the binding energies of O1s and C1s peaks and to normalize the spectra, when required. O1s and C1s peaks were measured with a photon energy of 620, 700, 875 and 1115 eV. Additional details on the fitting procedure are available in the Supporting Information file.

(vi) Field Emission Gun Scanning Electron Microscopy of the thin films was performed on a Hitachi SU-70 at 5 kV.

Acknowledgements:

This work was supported by the Director, Office of Science, Office of Basic Energy Sciences, Chemical Sciences, Geosciences, and Biosciences Division, under the Department of Energy Contract No. DE-AC02-05CH11231. Funding from the same contract for the ALS and beamline 11.0.2 is also acknowledged. D.P.D. thanks the Fonds national de la Recherche Scientifique for the mobility grant which made this collaboration possible. UPMC, CNRS and Collège de France are also acknowledged.

Supporting Information Available: FEG-SEM observation of the thin films and additional details about the fitting procedure.

Table of content graphic

References

[1] K. Aika, H. Hori, A. Ozaki, *J. Catal.* **1972**, *27*, 424–431.
[2] C. Fernández, C. Sassoye, D. P. Debecker, C. Sanchez, P. Ruiz, *Appl. Catal. A Gen.* **2014**, *474*, 194–202.
[3] P. Gallezot, S. Chaumet, A. Perrard, P. Isnard, *J. Catal.* **1997**, *168*, 104–109.
[4] D. P. Debecker, B. Farin, E. M. Gaigneaux, C. Sanchez, C. Sassoye, *Appl. Catal. a-General* **2014**, *481*, 11–18.
[5] M. C. J. Bradford, M. A. Vannice, *Catal. Rev.* **1999**, *41*, 1–42.
[6] Y. D. Kim, H. Over, G. Krabbes, G. Ertl, *Top. Catal.* **2000**, *14*, 95–100–100.

[7] D. Crihan, M. Knapp, S. Zweidinger, E. Lundgren, C. J. Weststrate, J. N. Andersen, A. P. Seitsonen, H. Over, *Angew. Chemie* **2008**, *120*, 2161–2164.
[8] D. Teschner, R. Farra, L. Yao, R. Schlögl, H. Soerijanto, R. Schomäcker, T. Schmidt, L. Szentmiklósi, A. P. Amrute, C. Mondelli, et al., *J. Catal.* **2012**, *285*, 273–284.
[9] G. Xiang, X. Shi, Y. Wu, J. Zhuang, X. Wang, *Sci. Rep.* **2012**, *2*, DOI 10.1038/srep00801.
[10] C. Mondelli, A. P. Amrute, F. Krumeich, T. Schmidt, J. Pérez-Ramírez, *ChemCatChem* **2011**, *3*, 657–660.
[11] M. A. A. Aziz, A. A. Jalil, S. Triwahyono, A. Ahmad, *Green Chem.* **2015**, *17*, 2647–2663.
[12] Q. Lin, X. Y. Liu, Y. Jiang, Y. Wang, Y. Huang, T. Zhang, *Catal. Sci. Technol.* **2014**, *4*, 2058.
[13] E. Zağli, J. Falconer, *J. Catal.* **1981**, *8*, 1–8.
[14] M. Prairie, A. Renken, J. G. Highfield, K. Ravindranathan, M. Grätzel, *J. Catal.* **1991**, *129*, 130–144.
[15] P. Panagiotopoulou, D. I. Kondarides, X. E. Verykios, *J. Phys. Chem. C* **2011**, *115*, 1220–1230.
[16] P. Szedlacsek, L. Guczi, M. Marwood, R. Doepper, A. Renken, *Appl. Catal. A Gen.* **1997**, *151*, 223–246.
[17] P. Ferreira-Aparicio, I. Rodríguez-Ramos, J. . Anderson, a Guerrero-Ruiz, *Appl. Catal. A Gen.* **2000**, *202*, 183–196.
[18] C. Sassoye, G. Muller, D. P. Debecker, A. Karelovic, S. Cassaignon, C. Pizarro, P. Ruiz, C. Sanchez, *Green Chem.* **2011**, *13*, 3230.
[19] M. Hävecker, R. W. Mayer, A. Knop-Gericke, H. Bluhm, E. Kleimenov, A. Liskowski, D. Su, R. Follath, F. G. Requejo, D. F. Ogletree, et al., *J. Phys. Chem. B* **2003**, *107*, 4587–4596.
[20] M. E. Grass, Y. Zhang, D. R. Butcher, J. Y. Park, Y. Li, H. Bluhm, K. M. Bratlie, T. Zhang, G. a Somorjai, *Angew. Chem. Int. Ed. Engl.* **2008**, *47*, 8893–6.
[21] S. Zafeiratos, F. Paloukis, G. Papakonstantinou, D. Teschner, M. Hävecker, E. Vass, P. Schnörch, a. Knop-Gericke, R. Schlögl, B. Moreno, *Catal. Today* **2010**, *157*, 250–256.
[22] A. Caballero, J. P. Holgado, V. M. Gonzalez-delaCruz, S. E. Habas, T. Herranz, M. Salmeron, *Chem. Commun. (Camb).* **2010**, *46*, 1097–9.
[23] M. E. Grass, M. Park, F. Aksoy, Y. Zhang, M. Kunz, Z. Liu, B. S. Mun, *Langmuir* **2010**, *26*, 16362–7.
[24] J. R. Renzas, W. Huang, Y. Zhang, M. E. Grass, D. T. Hoang, S. Alayoglu, D. R. Butcher, F. F. Tao, Z. Liu, G. a Somorjai, *Phys. Chem. Chem. Phys.* **2011**, *13*, 2556–62.
[25] M. Behrens, F. Studt, I. Kasatkin, S. Kühl, M. Hävecker, F. Abild-Pedersen, S. Zander, F. Girgsdies, P. Kurr, B.-L. Kniep, et al., *Science* **2012**, *336*, 893–7.
[26] S. Carenco, A. Tuxen, M. Chintapalli, E. Pach, C. Escudero, T. D. Ewers, P. Jiang, F. Borondics, G. Thornton, A. P. Alivisatos, et al., *J. Phys. Chem. C* **2013**, *117*, 6259–6266.
[27] S. Carenco, C.-H. Wu, A. Shavorskiy, S. Alayoglu, G. A. Somorjai, H. Bluhm, M. Salmeron, *Small* **2015**, *11*, 3045–3053.
[28] S. Carenco, *Chem. Eur. J.* **2014**, *20*, 10616–10625.
[29] K. Qadir, S. M. Kim, H. Seo, B. S. Mun, F. A. Akgul, Z. Liu, J. Y. Park, *J. Phys. Chem. C* **2013**, *117*, 13108–13113.
[30] M. Kuemmel, J. Allouche, L. Nicole, C. Boissière, C. Laberty, H. Amenitsch, C. Sanchez, D. Grosso, *Chem. Mater.* **2007**, *19*, 3717–3725.
[31] M. Faustini, D. Grosso, *Comptes Rendus Chim.* **2015**, DOI 10.1016/j.crci.2015.05.011.
[32] M. Faustini, A. Capobianchi, G. Varvaro, D. Grosso, *Chem. Mater.* **2012**, *24*, 1072–1079.
[33] D. Frank Ogletree, H. Bluhm, E. D. Hebenstreit, M. Salmeron, *Nucl. Instruments Methods Phys. Res. Sect. A Accel. Spectrometers, Detect. Assoc. Equip.* **2009**, *601*, 151–160.
[34] C. Wu, M. S. J. Marshall, M. R. Castell, *J. Phys. Chem. C* **2011**, *115*, 8643–8652.
[35] N.□; Fairley, **2003**, Casa Software version 2.3.15, Ltd., Teighnmouth, D.
[36] D. J. Morgan, *Surf. Interface Anal.* **2015**, *47*, 1072–1079.
[37] P. J. Cumpson, M. P. Seah, *Surf. Interface Anal.* **1997**, *25*, 430–446.
[38] W. S. M. Werner, *Surf. Interface Anal.* **2001**, *31*, 141–176.
[39] S. Tanuma, C. J. Powell, D. R. Penn, *Surf. Interface Anal.* **2003**, *35*, 268–275.
[40] R. Madon, E. Iglesia, *J. Catal.* **1993**, *139*, 576–590.
[41] W. Wang, S. Wang, X. Ma, J. Gong, *Chem. Soc. Rev.* **2011**, *40*, 3703–27.
[42] B. Ohtani, O. O. Prieto-Mahaney, D. Li, R. Abe, *J. Photochem. Photobiol. A Chem.* **2010**, *216*, 179–182.
[43] M. Kuemmel, C. Boissiere, L. Nicole, C. Laberty-Robert, C. Sanchez, D. Grosso, *J. Sol-Gel Sci. Technol.* **2008**, *48*, 102–112.

[44] Y. Kaga, Y. Abe, H. Yanagisawa, *Surf. Sci. …* **1999**, *6*, 68–74.
[45] D. Li, N. Ichikuni, S. Shimazu, T. Uematsu, *Appl. Catal. A Gen.* **1999**, *180*, 227–235.
[46] K. Qadir, S. H. Joo, B. S. Mun, D. R. Butcher, J. R. Renzas, F. Aksoy, Z. Liu, G. a Somorjai, J. Y. Park, *Nano Lett.* **2012**, *12*, 5761–8.
[47] C. Elmasides, D. I. Kondarides, S. G. Neophytides, X. E. Verykios, *J. Catal.* **2001**, *198*, 195–207.
[48] D. E. Starr, H. Bluhm, *Surf. Sci.* **2013**, *608*, 241–248.
[49] C. Sassoye, C. Laberty, H. Le Khanh, S. Cassaignon, C. Boissiere, M. Antonietti, C. Sanchez, *Adv. Funct. Mater.* **2009**, *19*, 1922–1929.